Electronic supplementary information for

Room-temperature near-infrared whispering-gallery-mode lasing from two-dimensional CdSe microplates

Lei Kong,[a] Yang Mi,*[a] Weizheng Liang,*[b] Sheng-Nian Luo[a]

[a]Key Laboratory of Advanced Technologies of Materials, Ministry of Education, School of Materials Science and Engineering, Southwest Jiaotong University, Chengdu, Sichuan 610031, P. R. China.
Email: miyang@swjtu.edu.cn

[b]The Peac Institute of Multiscale Sciences, Chengdu, Sichuan 610031, P. R. China.
Email: wzliang@pims.ac.cn

Contents

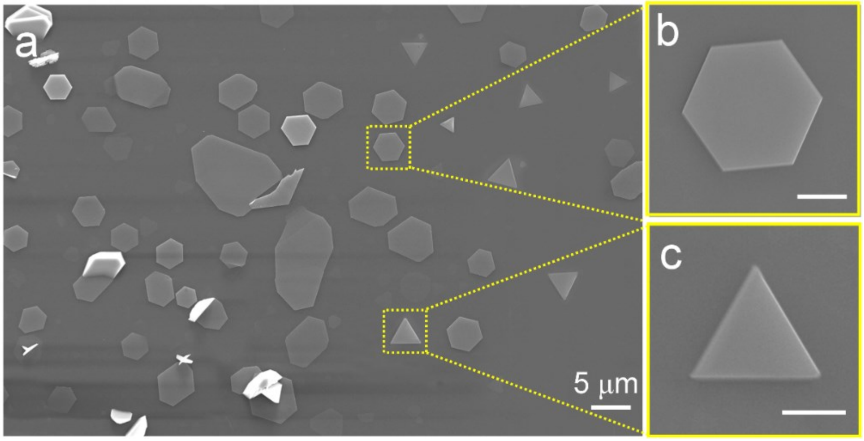

Fig. S1 (a) Typical SEM image of the CdSe MPs on a mica substrate. The scale bar denotes 5 μm. (b, c) The magnifed SEM images of the hexagonal and triangular CdSe MPs. The scale bars are both 2 μm.

The morphologies of the CdSe MPs were further characterized via scanning electron microscopy (SEM), as shown in **Fig. S1**. It can be seen that most of the MPs are featured with well-defined hexagonal or triangular shapes. **Fig. S1b, c** show the magnified SEM images of individual hexagonal and triangular CdSe MPs, respectively. It can be clearly seen that both of the hexagonal and triangular MPs present a highly smooth top surface with extremely low surface roughness, which can e□ectively reduce the scattering loss as well as the contaminant loss. Such smooth edges in the magnified SEM images suggest the smooth side surfaces of the CdSe MPs.

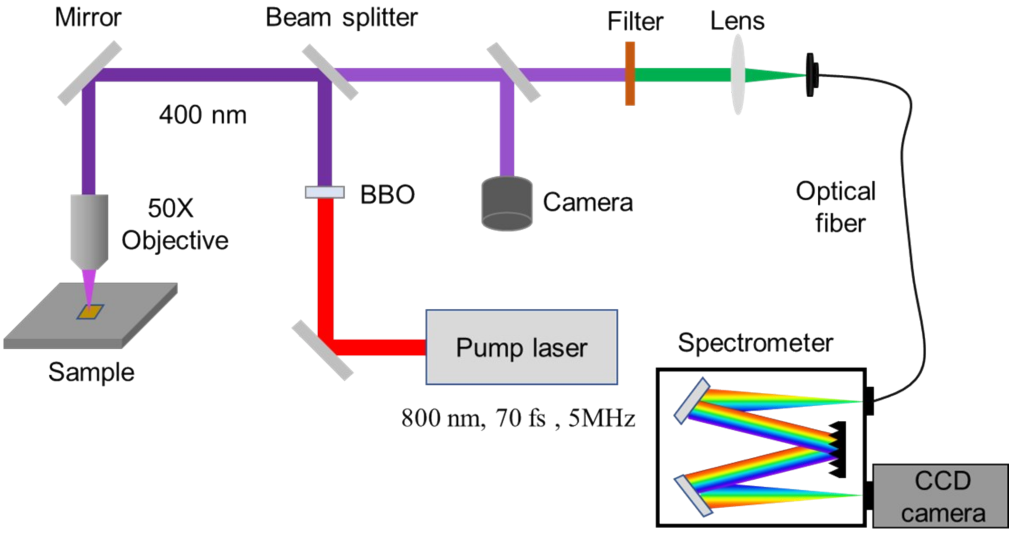

Fig. S2 Setup for photoluminescence and lasing characterization with a home-built micro-photoluminescence spectrometer.

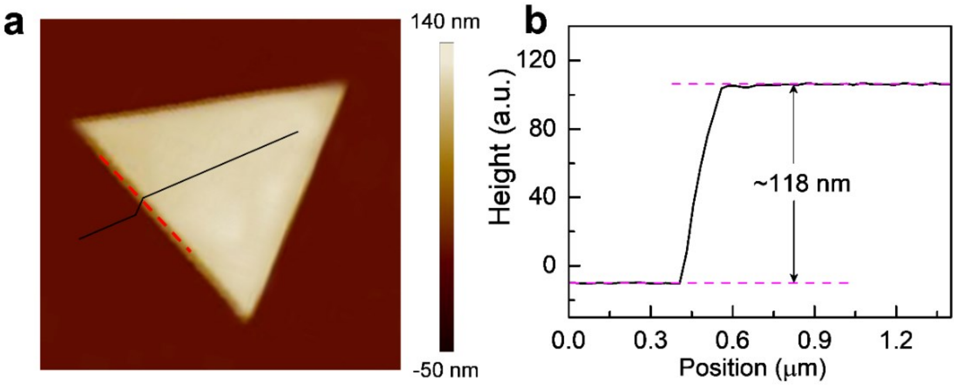

Fig. S3 The AFM image and the corresponding height profile of the typical triangular CdSe MP in the inset of Fig. 2d, showing a plate height of ~118 nm.

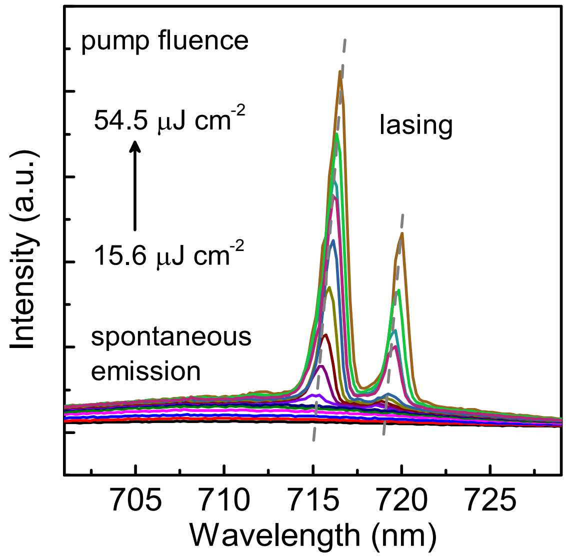

Fig. S4 Magnified emission spectra of the typical CdSe hexagonal MP at different optical pump fluences from 15.6 to 54.5 μJ/cm^2, which shows the red shift of the lasing peak with increasing pump fluence.

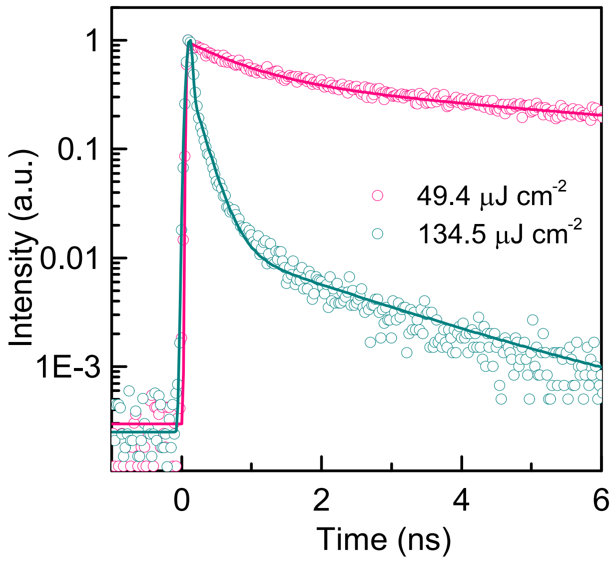

Fig. S5 The decay profiles of the emission from a typical triangular CdSe MP measured under the pump fluence of 49.4 and 134.5 μJ/cm^2, respectively. Solid lines are the fitted results.

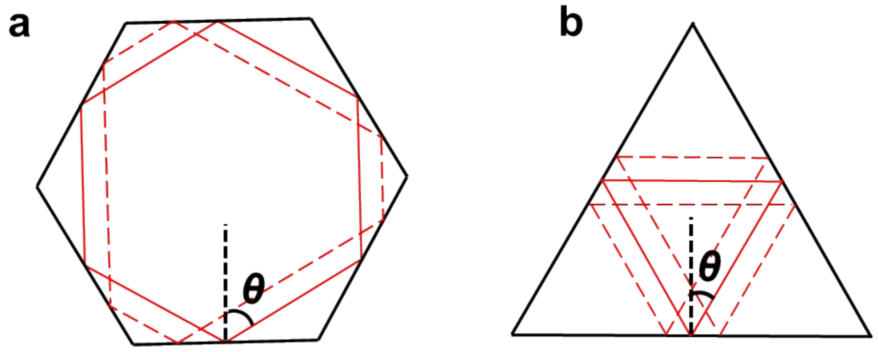

Fig. S6 (a) The hexagonal and (b) triangular periodic orbits in the hexagonal and triangular microcavities, respectively. The solid lines and dashed lines indicate the ray trajectories connecting the sides and the other ray trajectories in the same orbit family with the same incident angles.

To give an intuitive description of WGMs, the semi-classical geometrical optical models[3] are introduced into the polygonal microcavities. **Fig. S6a, b** show the light can be totally reflected at the cavity sides both in hexagonal ($\theta = \pi/3$) and triangular ($\theta = \pi/6$) microcavities. The solid line indicates the ray trajectory connecting the midpoints of adjacent sides, whereas the dashed line indicates one ray trajectory within the same orbit family with equal orbit length and incident angle. However, the incident angles in polygonal cavities with finite sizes are not exactly $\pi/3$ or $\pi/6$, considering the transverse distribution of the periodic orbits. For a light ray with an initial incident angle (θ) in hexagonal cavity, the subsequent incident angle is $2\pi/3-\theta$. Since both of the incident angles are much larger than the critical angle θ_c (24.5°), strong light confinement can be achieved via total internal reflection in hexagonal cavity with little radiation loss. In the case of the triangular cavity, the subsequent incident angle is $\pi/3-\theta$. Only when $\theta > \theta_c$ and $\pi/3-\theta > \theta_c$ is simultaneously satisfied, all the incident angles can be kept above the total internal reflection condition. This means the deviation of incident angle ($\Delta\theta$) in triangular cavity may result in evident boundary wave and pseudo-integrable leakage, which is due to the small incident angle around $\pi/6$ (near θ_c).

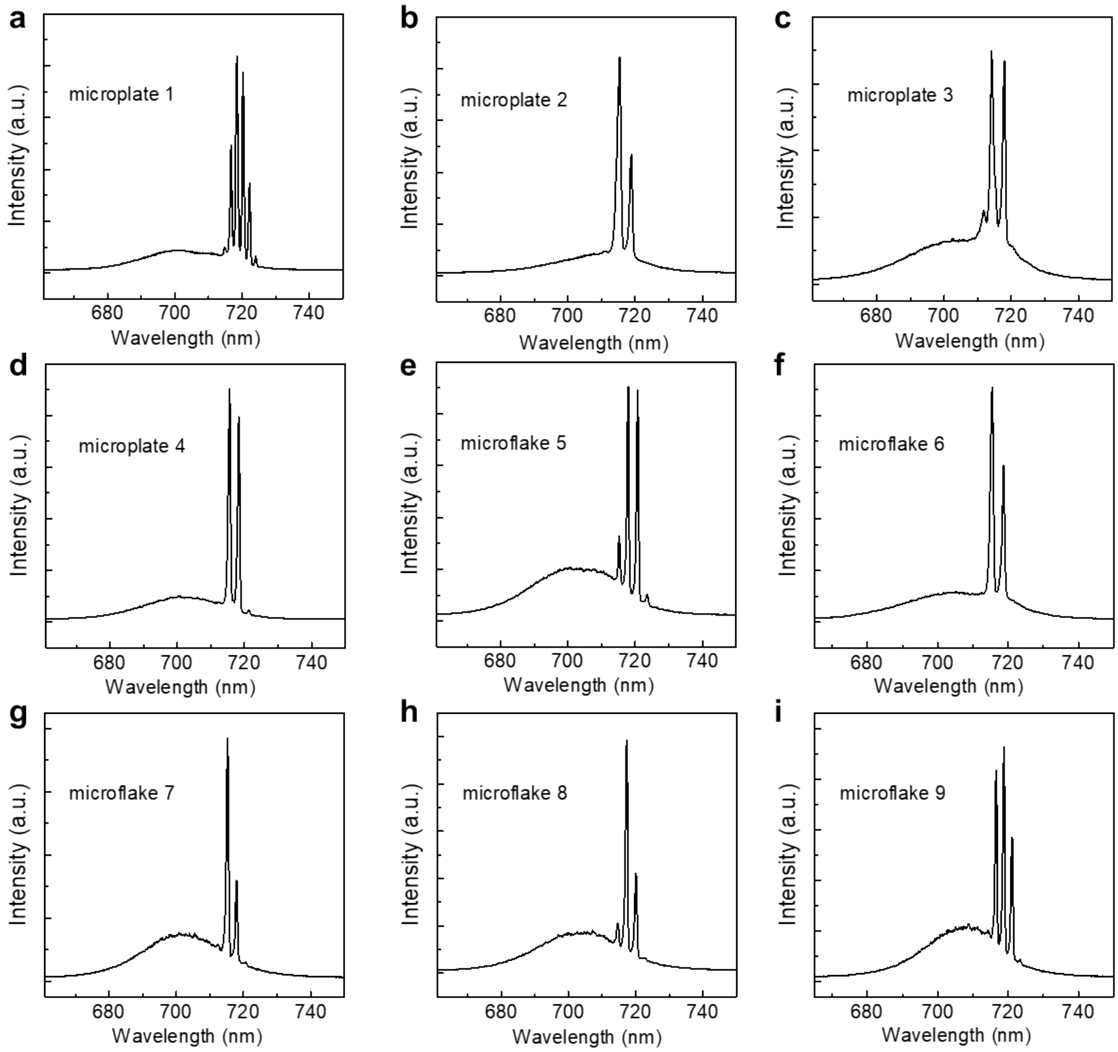

Fig. S7 Lasing spectra of several hexagonal CdSe MPs with different edge lengths, showing distinguishable free spectral range ($\Delta\lambda$).

TRPL Decay profile fitting

In our experiment, the Gaussian response function convoluted with bi-exponential model was used to fit the TRPL decay traces in Fig. 3 and Fig. S2, the TRPL traces I(t) can be described by the Equation (1) below,

$$I(t)=A_1\, exp\,(-t/\tau_1) + A_2\, exp\,(-t/\tau_2) \qquad (1)$$

where A_1 and τ_1 (A_2 and τ_2) represent the amplitude and lifetime of the fast (slow) decay components ($\tau_1 < \tau_2$), respectively.

Table S1. Fitting parameters for TRPL decay profiles of a typical CdSe MP at different pump fluences in Fig. 3a using the Gaussian response function convoluted with the monoexponential and di-exponential decay functions.

Pump fluence (μJ/cm^2)	Decay time (ps)	Amplitude (%)
19.5	τ=2604±58	100
39.1	τ_1=87.2±3.4	71.3
	τ_2=684.5±43.2	28.7
42.3	τ_1=45.1±2.6	84.2
	τ_2=426.3±24.4	15.8
46.2	τ_1=31.2±1.8	98.9
	τ_2=264.6±15.5	1.1

Table S2. Fitting parameters for TRPL decay profiles of triangular CdSe MP at different pump fluences in Fig. S5 using the Gaussian response function convoluted with the monoexponential and di-exponential decay functions.

Pump fluence (μJ/cm^2)	Decay time (ps)	Amplitude (%)
49.4	τ=2528±53	100
134.5	τ_1=42.6±3.5	85.6
	τ_2=405.3±21.2	14.4